IB Physics Extended Essay:

How does the lift force of asymmetrical and symmetrical airfoils vary depending on their top to bottom thickness ratio?

IBIS Personal Code: ------

Ivan Baklanov

3862 words

November 22, 2020

Table of Contents

Introduction

Context, Background and Methodology

I have been moving around the world my whole life, establishing partial lives in 4 countries. I tend to visit friends and family often by plane, and have always been fascinated at how such a large and heavy piece of machinery can take off into the sky with seamless effort. When I was younger, I looked at airplanes as if they were made out of magic. I am still very intrigued by this now that I am older, and aerospace mechanical engineering is my goal. I have chosen my Extended Essay as a way to follow my curiosity and understand part of the magic which makes flying possible.

That being said, I cannot investigate the whole of an aircraft due to safety concerns and lack of equipment. Instead, I have chosen to investigate one of the most crucial elements of an aircraft: the wing. This part is also known as an airfoil, which is the term I will be using throughout this paper. There are four essential forces in an aircraft, illustrated in Figure 1 (*Four Forces of Flight*).

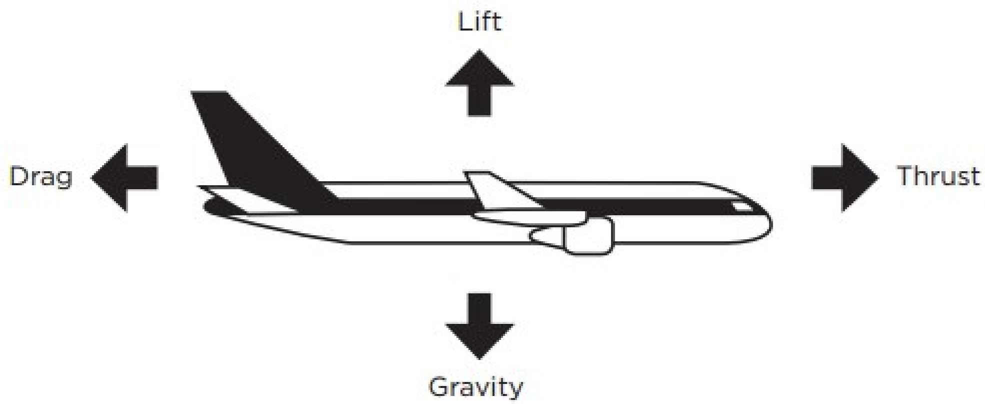

Figure 1: The four forces of flight.

I have chosen to investigate the lift force of an airfoil, as it is what allows for flight. In order to do this, I will keep the airfoil fixed to a load cell and provide airflow to it. This eliminates thrust (because the airfoil is not moving forwards/backwards) and weight, as I will tare (set to 0) the weight, so that the only force recorded is the lift, regardless of the weight[1]. Although this methodology does not cancel out the drag force, it makes the lift force easier to analyze. I will not be quantifying or analyzing the drag force.

The main theoretical background for this experiment is based Bernoulli's equation (Tsokos, 2014), which states that (for an incompressible fluid):

$$p_1 + \tfrac{1}{2}\rho v_1^2 + \rho g z_1 = p_2 + \tfrac{1}{2}\rho v_2^2 + \rho g z_2$$

Where ρ is the density of the fluid [kgm^{-3}], v is the speed of the fluid [ms^{-1}], g is the gravitational acceleration due to gravity [ms^{-2}] (conventionally, this is 9.81 ms^{-2} on the Earth's surface), z is the height from a reference source [m], and p is the pressure exerted by the fluid to surrounding sources [Pa].

[1] I confirmed this idea by observing how the lift force did not change when weight is added to an airfoil.

This equation shows us that there is a relationship between fluid speed and the pressure exerted by said fluid, such that a slower fluid creates a larger pressure, and a faster pressure creates a relatively weaker pressure. This equation also deducts that the greater the change in altitude, the faster an incompressible fluid is forced to flow; hence a smaller pressure is produced. When applied to an airfoil (Tsokos, 2014):

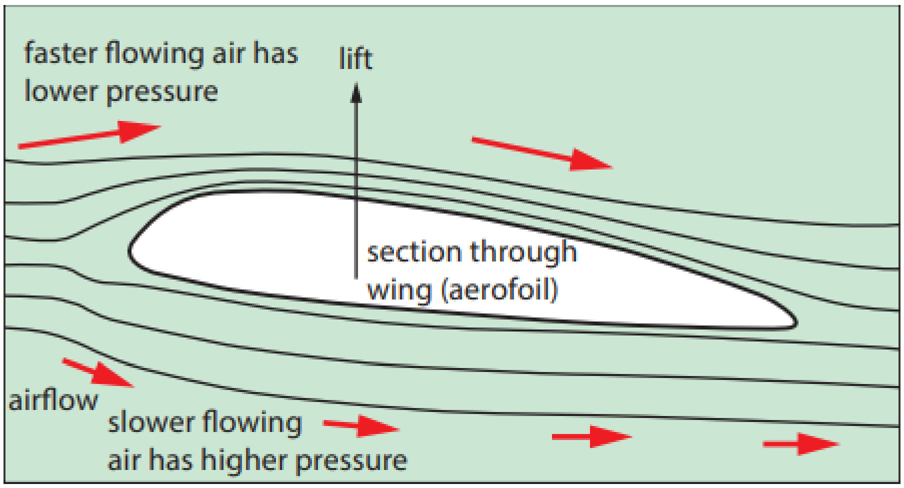

Figure 2: The Bernoulli effect on an airfoil. The terms airfoil and aerofoil are interchangeable.

I will be using both asymmetrical and symmetrical airfoils. An important part of an airfoil is the chord, which is the base line upon which everything else is modelled (Hall, 2018). Other measurements are often relative to this line in **percent chord** (percentage of the chord length). See Figure 2.5 (Hall, 2018).

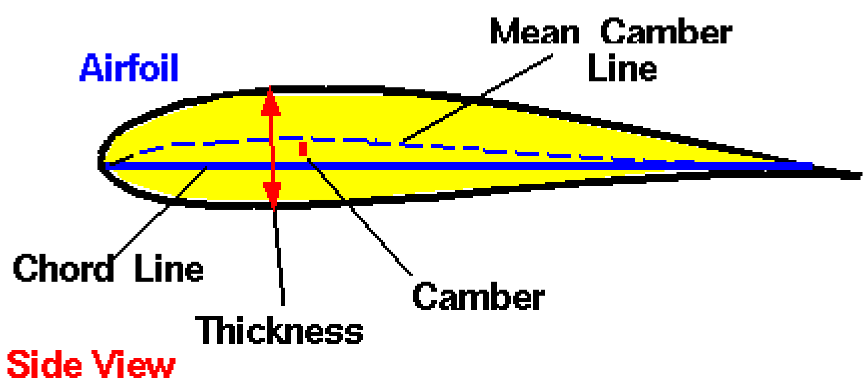

Figure 2.5: Parts of an airfoil. Note that the Mean Camber Line and Camber apply to a different type of airfoil, and will not be taken into account in this investigation.

I will be splitting the maximum thickness into the top and bottom maximum thickness, both relative and perpendicular to the chord. The ratio between these thicknesses will be my independent variable[2], and the lift force will be the recorded (dependent) variable. Relating once again to the Bernoulli equation, I will be keeping density and gravitational acceleration controlled and constant. As the height (z) changes with the varying thickness ratio, the pressure will differ, contributing to the distinct lift force measured.

Research Question

I can now state that my research question is:

"How does the lift force of asymmetrical and symmetrical airfoils vary depending on their top to bottom thickness ratio?"[3]

Airfoil Design

Two-Dimensional Design

When choosing the design and measurements for the airfoil, I first looked specifically at the chord and thickness. I chose to use 5 different airfoils so that the values at either end of my ratio samples (extremes) have a big contrast whilst still having 3 in-between points, showing a more accurate change in lift force. Furthermore, the materials and time needed to create each airfoil is significant, and the creation of a larger quantity would hinder the research, as time will be lost.

I chose the smallest ratio to be of 1:1, a symmetrical airfoil. Any ratio smaller than this would cause an 'upside-down' airfoil. The largest maximum thickness will be of 32% chord, as this leaves plenty of space for contrast between top and bottom thickness without being too thick.

[2] From now on, I will use the term 'thickness ratio' to mean the top to bottom thickness ratio.
[3] The definition and quantification of these terms are to be discussed in later sections.

Splitting this into top & bottom thickness (for a 1:1 ratio airfoil), I got 16% chord for each thickness, located at 30% chord (*Designing Smooth Symmetrical Airfoil Wings* 2016). Note that so far, all the dimensions are **relative** to the chord, and will be quantifiable once the chord is defined.

I chose for the other extremum to be a 6:1 ratio, as this provides a large contrast without making the bottom thickness negligible. When choosing the other three ratios I used a logarithmic scale by finding 3 points equidistant from $\log_{10} 1$ to $\log_{10} 6$ and converting them back to the linear scale and finding the nearest fraction to those integers. This logarithmic choosing method helps visualize the data when plotted, as the values will not be evenly spread out on the thickness ratio axis. Finally, I got these ratios:

1:1 25:16 5:2 4:1 6:1

All relative measurements being established, I chose the chord length to be 100 mm, making 1% chord translates directly to 1 mm. I have designed the airfoils with Adobe Photoshop (Figure 3, on following page) on a letter-size paper. When printed, the designs are to scale, so there is no need to use imprecise hand-made sketches.

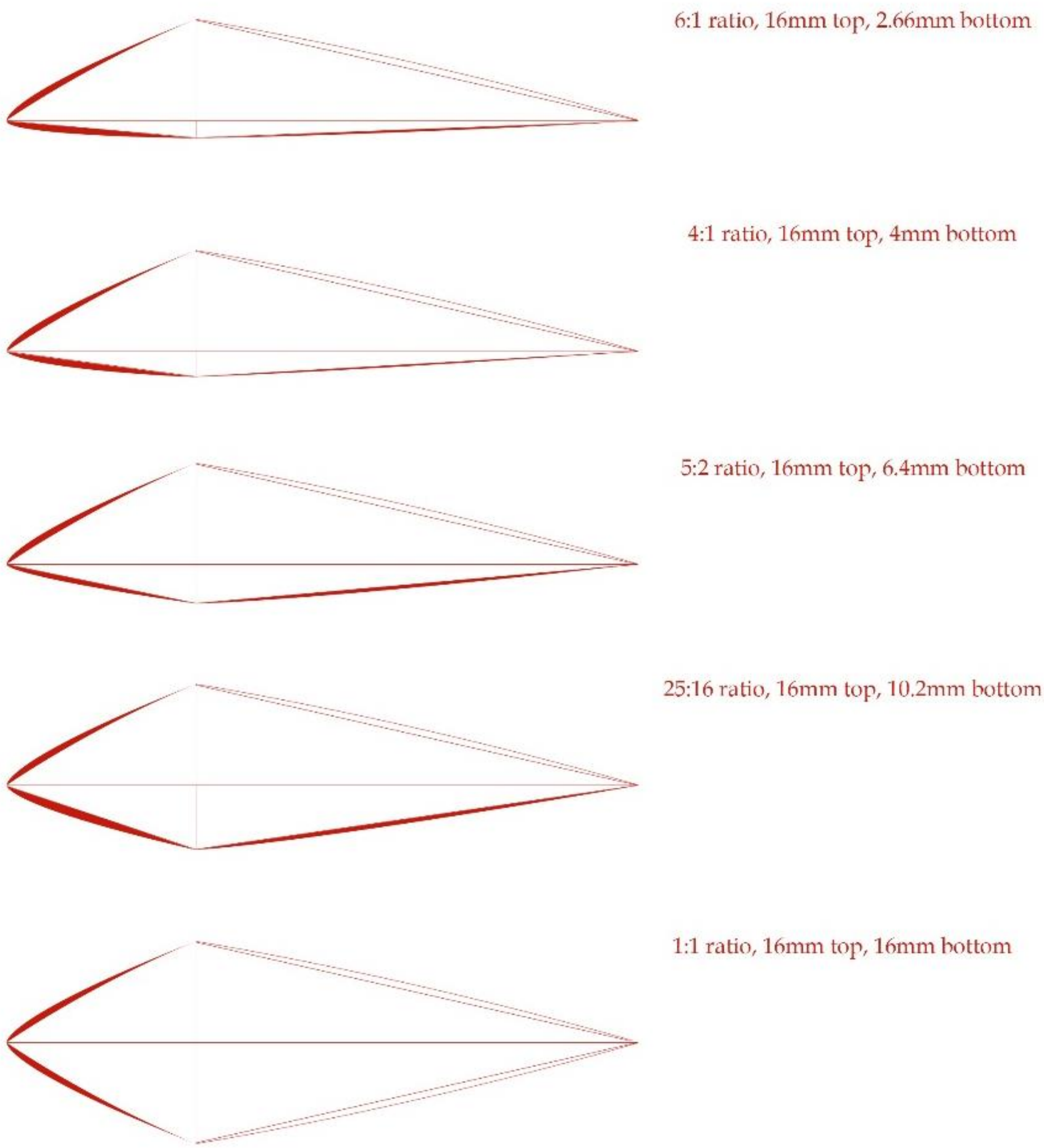

Figure 3: Airfoil designs with ratio and measurements. The horizontal line is the chord, and the vertical is the maximum thickness.

Depth

The ‘depth’ of an airfoil is known as its span. One of the ways to define the wing span is by using the following equation (Hall, 2018):

s = AR * c

where s is the wingspan, AR is the aspect ratio, and c is the chord length.

In order to find the span, I need to use a known aspect ratio. I chose to use the aspect ratio of the Piper Cherokee, an airplane commonly considered to be the ‘norm’, which has an AR of 5.63 (*Designing Smooth Symmetrical Airfoil Wings* 2016). This is for the whole wing span, and I am only interested in a single airfoil, meaning the AR becomes 2.815. Rounded up to 2.82, this makes each airfoil’s span 282mm (2.82 * 100mm).

Experimental Setup

Making of Airfoils

I chose to create the airfoils by cutting blocks of EPS insulation foam into the desired shape with the help of wooden molds. In order to do this, I created and used a hot wire tool, which consists of a nichrome resistance wire tensed up and connected to a power supply. When turned on, the nichrome wire heats up without burning and slices through the foam with a clean cut. This construction is shown in Figure 4 on the next page.

Figure 4: Hot wire construction for cutting foam into airfoils. Insulation tape provides protection against heat and electricity.

Figure 5 shows the airfoils once cut out with a protective respiratory mask. The measurements of each of the airfoils is negligibly different from the original design's dimensions and have an uncertainty of (+/-) 0.5mm for each measurement.

Figure 5: Cut out foam airfoils with labelled ratios.

After cutting out the airfoils, I noticed there were some discrepancies in the surface in the form of either a non-smooth cut caused by the glue used between layers, or a slight concave at the tailing edge of the airfoil.

Environmental Concern

While EPS insulating foam is not good to the environment because of the Greenhouse Gases released during its manufacturing, it is better than other insulating foams, CFCs in particular (Wilson, 2016). The remaining airfoils will either be handed to an environmentally-responsible recycling/waste-disposing center, or used for alternate projects. Any unused insulation foam will be used for practical insulation purposes.

Wind Tunnel

Diffuser + Airflow Straightener

The diffuser (Figure 6) is arguably the most important part of the wind tunnel as it concentrates the airflow and gives it time to straighten out to become more laminar (*How to Build and Use a Subsonic Wind Tunnel* 2020). Inside the diffuser is an airflow straightener (Figure 7) consisting of cylindrical tubes to help disperse the airflow more evenly and laminarly[4].

Figure 6: Diffuser

Figure 7: Airflow straightener

Motor/Propelling Mounting and Safety

The source of wind comes from a propeller attached to a motor connected to a power supply and an RPM controller. The power supply and any exposed wires are very dangerous due to high

[4] In unrecording testing, I noticed how the lift force of the airfoil had a smaller standard deviation when the airflow straightener was put in place.

voltage and current. To prevent any injury or death, any conducting material was covered in an insulating coating.

I added a metal shield around the propeller so any malfunction will not fly into open space, but either hit the wall or enter the diffuser. The propeller is tightly secured onto the motor, and the motor is securely mounted and clamped. I added stabilizers and clamped the entire construction to a heavy table to decrease the intensity of vibrations. Figure 8 shows this construction.

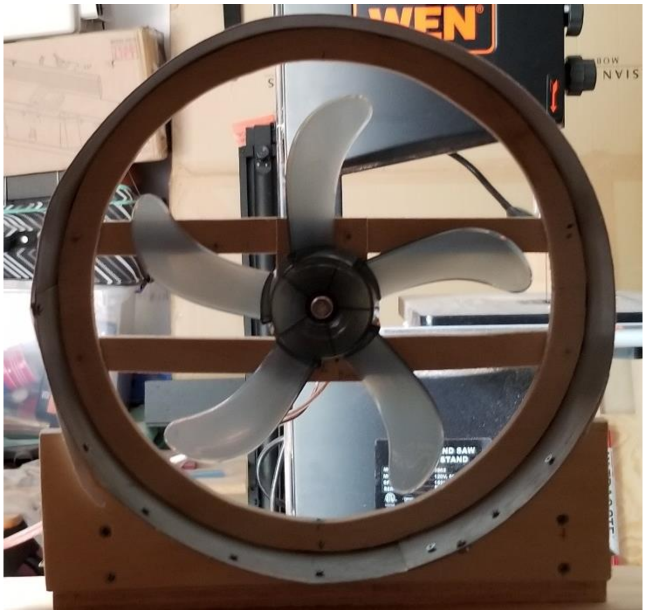

Figure 8: Propeller securely attached to motor and clamped down

Test Chamber

The test chamber is a wooden box allowing enough space for proper wind flow, and where the airfoil is mounted. It has a clear side to see the setup and measure the angle of attack relative to the chord, as well as a detachable top plank to make adjustments and set up the airfoil (Figure 9).

Inside of the test chamber, there are two guiding frames, one wooden and one clear, which are used to help the airfoil stay in place. This mechanism is not intended to fix the airfoil stiff, but rather to stop it from vibrating, which leads to more accurate measurements[5].

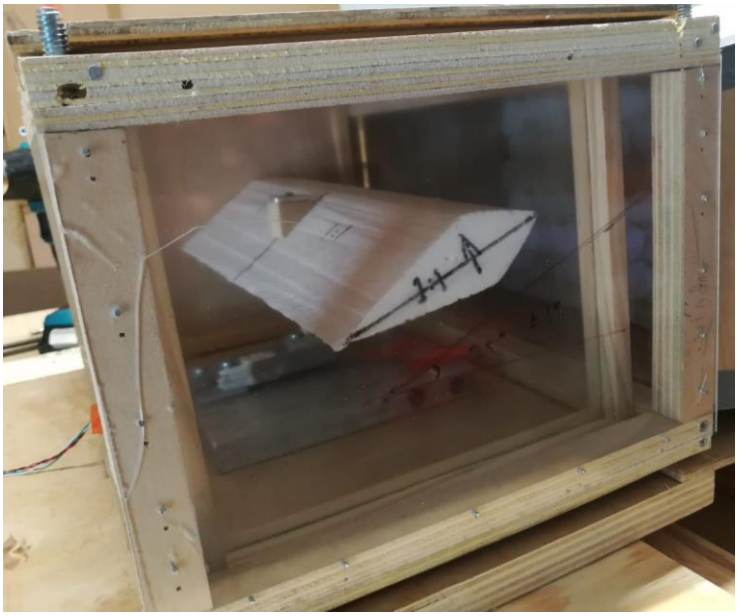

Figure 9: Test chamber with attached airfoil

Load Cell and Lift Force Recording

I used a load cell to measure the lift force. This is a device which measures the force applied to one of its sides. It uses fragile resistors so spacers were used during mounting (*HX711 Load Cell Amplifier Interface with Arduino* 2016). On the measuring side, a securely mounted wooden stick is attached to a screw and goes into the airfoil, which is then clamped with an angle of attack fixer[6]. Refer to Figure 10. The load cell is then attached to a used heavy metal plate and glued so that the screw is centered in the test chamber.

[5] Through un-recorded experimentation, I noticed that before these frames were added the lift force for any airfoil was extremely low, and very close to 0. It was visually distinguishable that this effect was caused because the airfoil was vibrating instead of pushing up.
[6] Explained in more detail in an upcoming section.

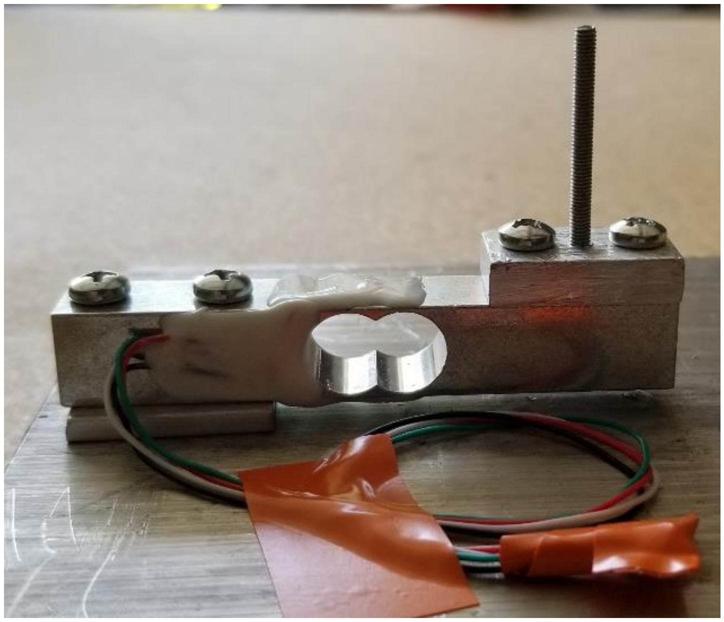

Figure 10: Load cell attached to heavy metal plate.

I used and modified an Arduino IDE code to calibrate and measure/record the force sensed (*HX711 Load Cell Amplifier Interface with Arduino* 2016). The precision of the load cell is, by default, (+/-) 0.05%. However, I got the load cell to measure a force precise to 1 gram after calibration with calibration weights. Hence, the uncertainty for each measurement is of (+/-) 0.5g.

It is impossible to record true natural data through electronic means but the fast sampling rate and low uncertainty, although do not make a fine line, are very precise (*Analog-to-digital converter* 2020). The recording of the measurements is done using a program called Tera Term which connects to an Arduino port.

Data Acquisition, Processing and Visualization

Measurement Devices

Here is a list of the measurement devices I used for each run:

1. Load cell (g)

2. Anemometer - wind speed (m/s)
3. Digital thermometer attached to motor (°C)
4. Multimeter (V)
5. Clamp-on ammeter (current) (A)
6. RPM Laser Tachometer (RPM)

Most measurements are non-essential for the analysis of the data, but served as a way for me to understand if there was any malfunction with the equipment or outlier runs.

Acquisition Routine

When recording the data, I made short (~ 30s) runs for each airfoil to prevent the motor from overheating. Each run had the following procedure:

1. Record the motor's temperature before run
2. Start the motor gradually
3. Record the motor's voltage, current, and RPM.
4. Start logging lift force (for ~30 s)
5. Record wind speed in output of test chamber
6. Stop logging
7. Gradually turn off motor
8. Record motor's final temperature
9. Wait for motor to cool close to the initial temperature
10. Start next run

Data Processing & Visualization

Once the raw data is recorded and stored, I processed and visualized the lift force data with GNU Octave (a multi-tool script software) scripts of my creation (*Function list*), allowing for graphing and data processing (i.e., mean force, standard deviation).

Experimental Data

Wind Speed Exploration

Description/Purpose

This exploration was used to find the optimal motor load for data gathering. There are several things to take into consideration:

1. Noise of data (i.e., dispersion through standard deviation)
2. Mean lift force produced
3. Signal-to-noise ratio (SNR) i.e., mean force / standard deviation

The concept of turbulence is an abstract one, and can only be somewhat quantified through the Reynolds number (Tsokos, 2014). Because it is virtually impossible to get true laminar flow, especially with wind, the noise of a dataset determines how turbulent the airflow is (i.e., the higher the noise, the more turbulent the wind). However, it is crucial to take the SNR into account, as a higher ratio gives a more accurate depiction of the true value under the set experimentational setup (*Signal-to-noise ratio* 2020).

For this exploration I only used the 4:1 airfoil at the Large angle of attack (25°)[7]. The wind speeds are determined by the motor load, which can be adjusted using the attached RPM controller.

[7] The angle of attack will be explored in an upcoming section.

I have decided to make the motor loads roughly (determined by my markings on the RPM controller) 50, 75, and 100% motor load.

Results

The following comparable (i.e., with the same axes) diagram summarizes the results of the wind speed exploration.

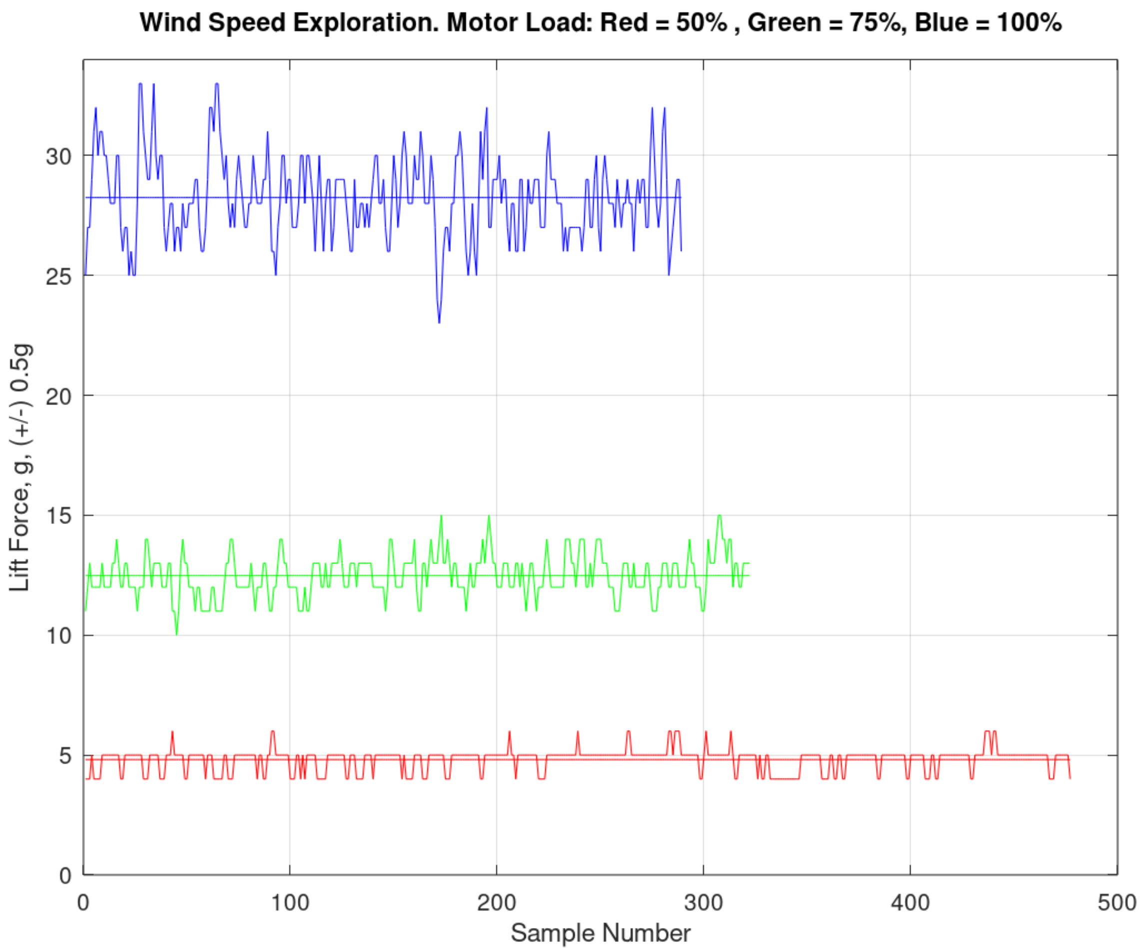

Figure 11: Comparable Wind Speed Exploration processed lift force data with mean lines. As the motor under 50% load is less likely to be damaged due to overuse, there are more samples in that dataset.

PARAMETERS	Motor Load 50%	75%	100%
Airfoil model	4:1	4:1	4:1
Angle of attack, deg (+/-) 1 deg	25	25	25
Wind speed, mean, m/s, (+/-) 0.1 m/s	1.9	2.8	3.8
Record length, samples	477	322	289
Lift force, mean, gram (+/- 1 g)	4.8 → 5	12.48 → 12	28.2 → 28
Percentage uncertainty relative to mean[8]	(+/-) 20%	(+/-) 9%	(+/-) 5%
Lift force noise (standard deviation), g	0.48	0.89	1.73
Signal-to-noise ratio	10.0	14.0	16.3

Table 1: Table displaying the data gathered for 50, 75, and 100% motor load

[8] i.e., mean (+/-) 1g turned to percentage

From the data above, it is evident that 100% motor is the most ideal. Although the turbulence at 100% motor load is 194% of the turbulence for 75% motor load (1.73/0.89 * 100% = 194%), the stronger signal-to-noise ratio, larger mean lift force, and smaller percentage uncertainty compensate for this flaw. This ultimately gives a more accurate portrayal of the average lift force under these set experimental circumstances. Furthermore, it is more consistent to set the RPM controller to 100%, as it will always be 100% (not accounting for the heating of the electrical components). This motor did not seem to show any danger of shattering under the influence of 100% load.

Lift Force Data Gathering & Processing

Description/Purpose:

After fixing which motor load I will be using for the measurements, the next step was to start taking the measurements for each airfoil themselves.

Angle of Attack

My original idea was to measure each airfoil parallel to the direction (0° angle of attack) of the airflow. However, after fixing the Angle of Attack (AOK - measured relative to the chord) to zero, the lift force measurements from the 5:2 airfoil was so negligibly low (around 3 g) that I decided to increase the lift force. This consequently improves the measurements' precision by lowering the percentage uncertainty. I achieved this by changing the AOK to a higher value. I chose to make the Medium (M) angle of attack 11.5° → 12°. To see how the results would change depending on the AOK, I also decided to take the same measurements on a Large AOK of 25° [9].

[9] From now on, the AOK described with an M stands for medium (15°), L for large (25°), and S for small (0°). The small AOK does not appear in this document, as it's lift force is negligible.

Aside from curiosity, this will also serve as a way to understand the **reproducibility** of this experimentation (i.e., how effective it is if replicated).

The uncertainty of the measurement for the AOK is of (+/-) 1°[10], as it was taken with a protractor, as displayed in Figure 12. However, this uncertainty is negligible, as the angle will be kept constant (therefore a controlled variable) and any slight change to it will not significantly affect the data, keeping it analyzable.

Figure 12: Setup used to confirm the angle of attack.

Figure 13: Angle of attack fixers. The 15° mark is the angle needed for the airfoil to level out, and read an AOK of 0°.

[10] The AOK is measured relative to the airfoil's chord.

Medium AOK

After collecting and processing data, the following graphs depict the results for each airfoil with an AOK of 12° (Medium).

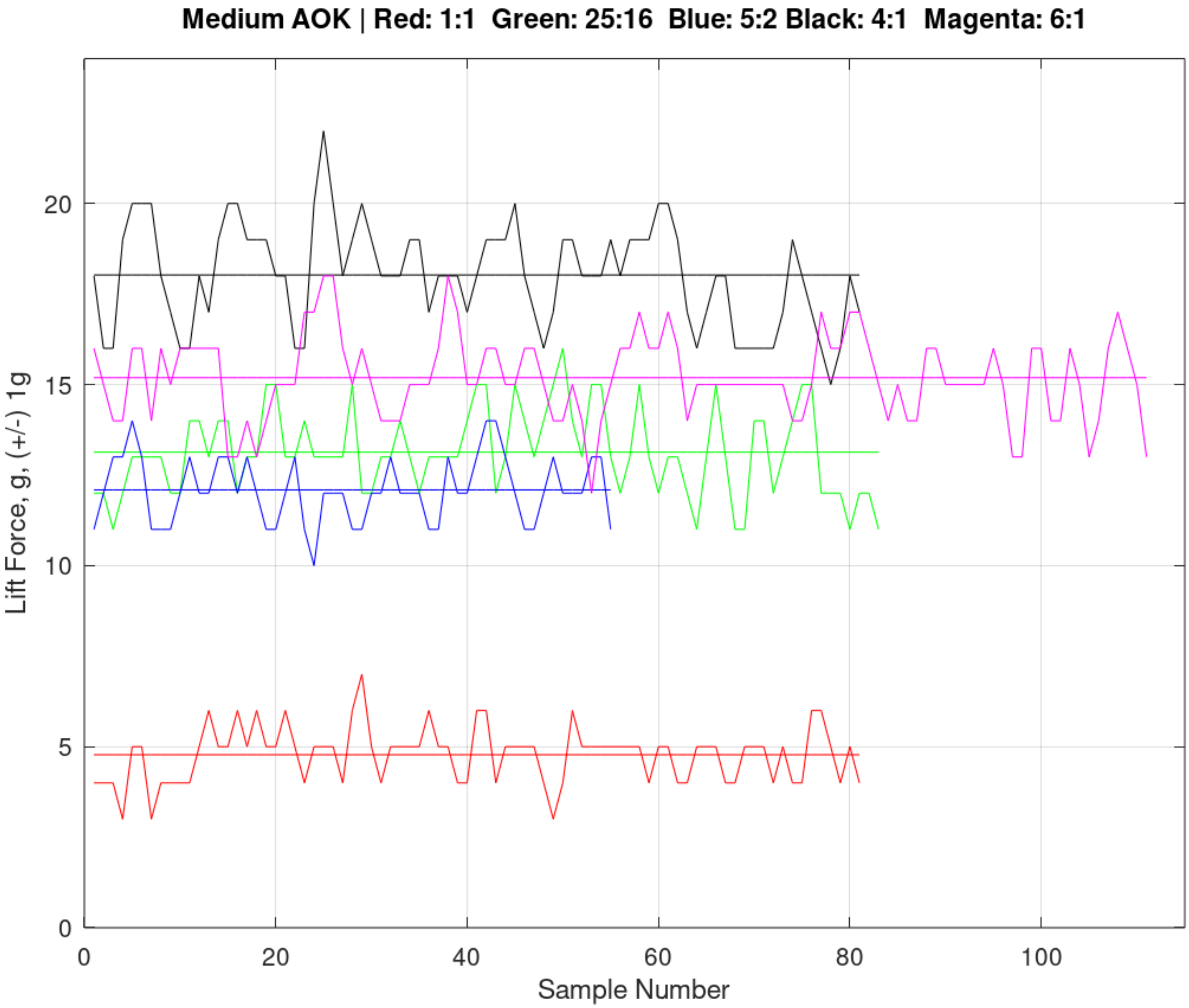

Figure 14: Comparable superimposed datasets for each airfoil under the Medium AOK with mean lines. In order from smallest to greatest mean force: 1:1, 5:2, 25:16, 6:1, 4:1

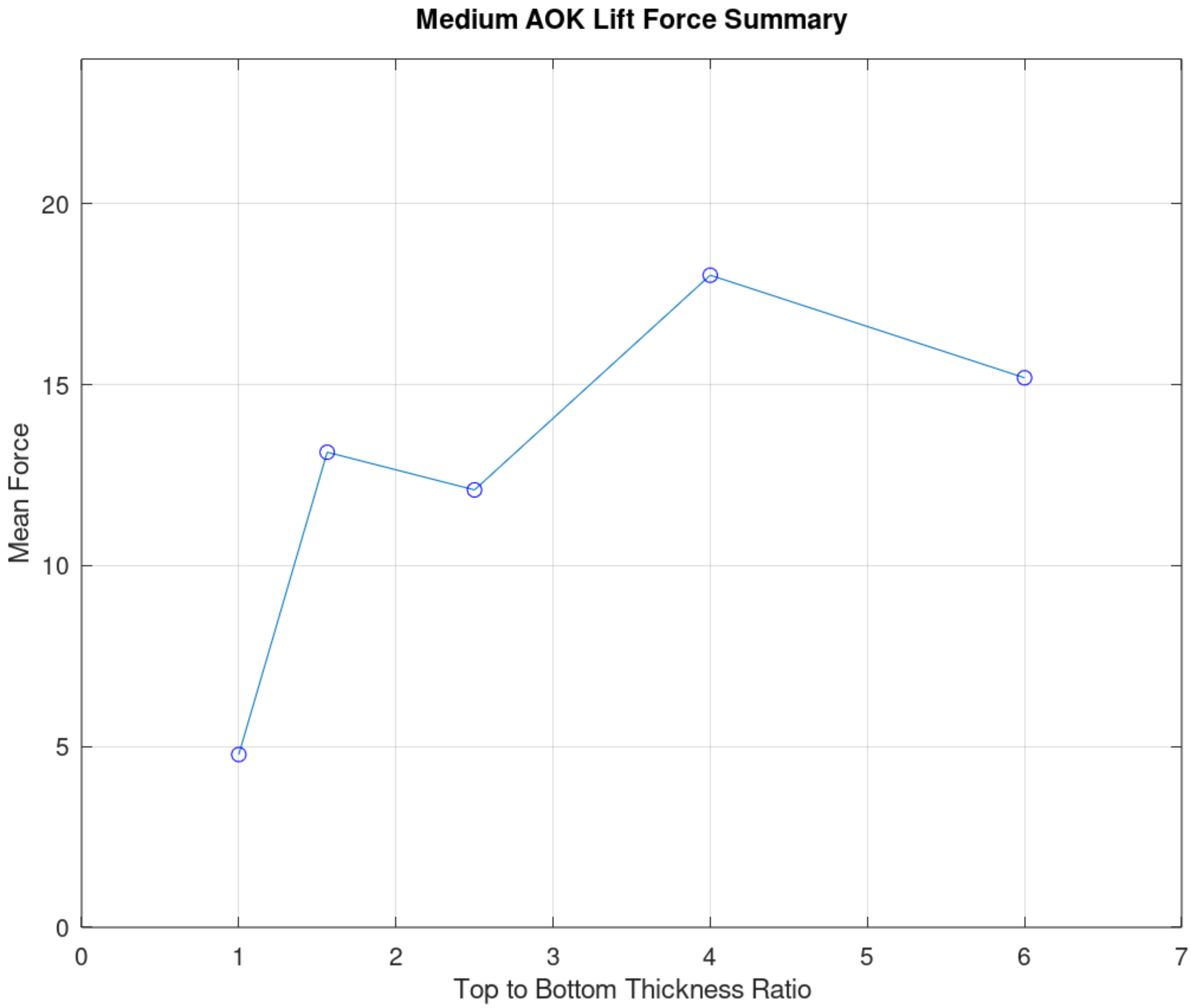

Figure 15: Summary of Medium AOK mean lift forces. The connecting lines are only used to facilitate interpretation of the graph, and do not possess any value; only the individual points for each measured airfoil ratio have a true value. The uncertainties for these measured values will be discussed in the Analysis.

	1:1	25:16	5:2	4:1	6:1
Mean Lift Force, g, (+/-)1g	4.7778 → 5	13.1325 → 13	12.0909 → 12	18.0247 → 18	15.1892 → 15
Standard Deviation, g	0.77	1.19	0.91	1.41	1.16
Signal-to-Noise Ratio	6.17	11.06	13.31	12.75	13.05

Table 2: Mean lift force, standard deviation, and signal-to-noise ratio (SNR) for each airfoil model under the Medium AOK.

Graphs continue on following page

Large AOK

After collecting and processing data, the following graphs depict the results for each airfoil with an AOK of 25° (Large).

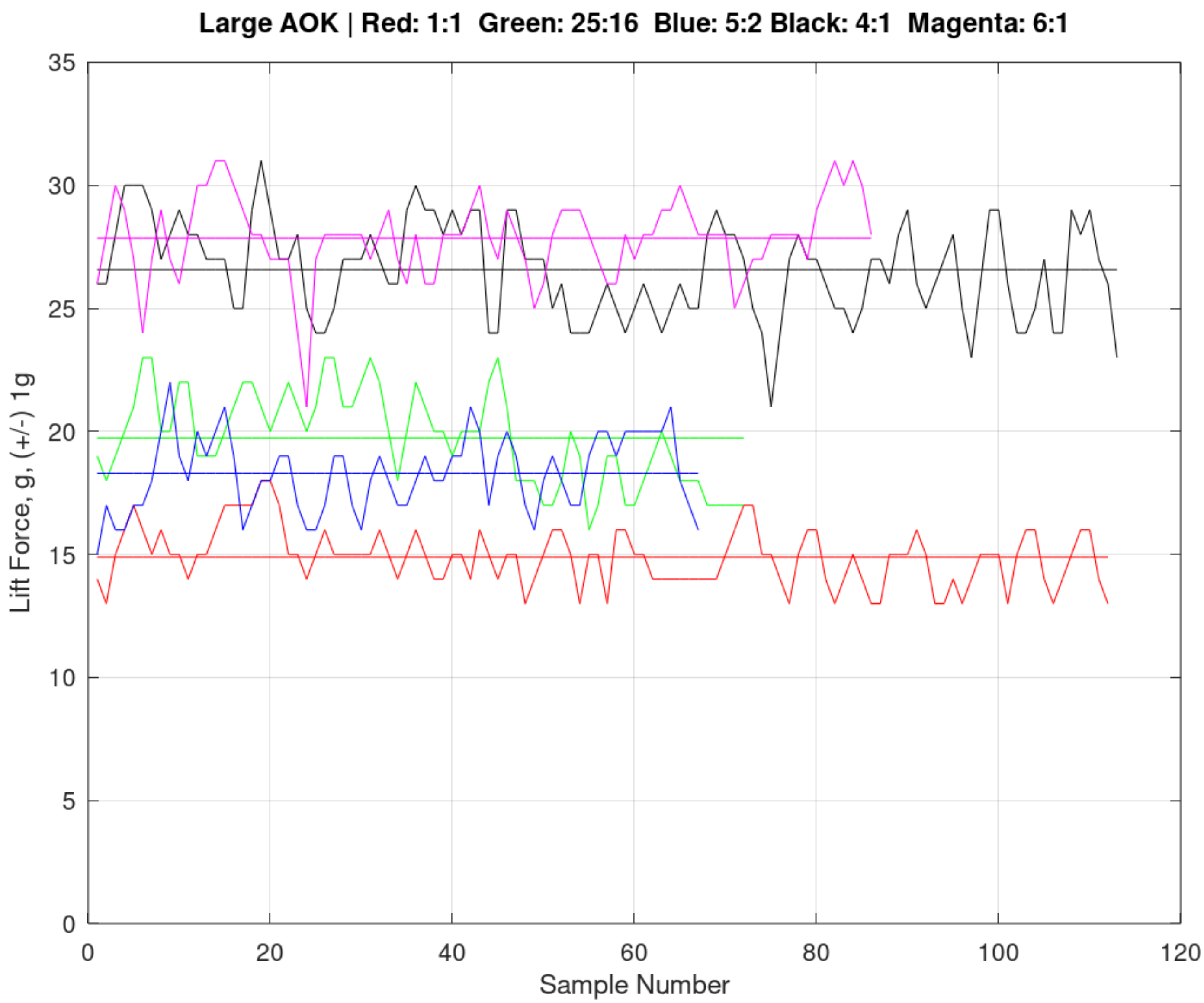

Figure 16: Comparable superimposed datasets for each airfoil under the Large AOK with mean lines. In order from smallest to greatest mean force: 1:1, 5:2, 25:16, 4:1, 6:1

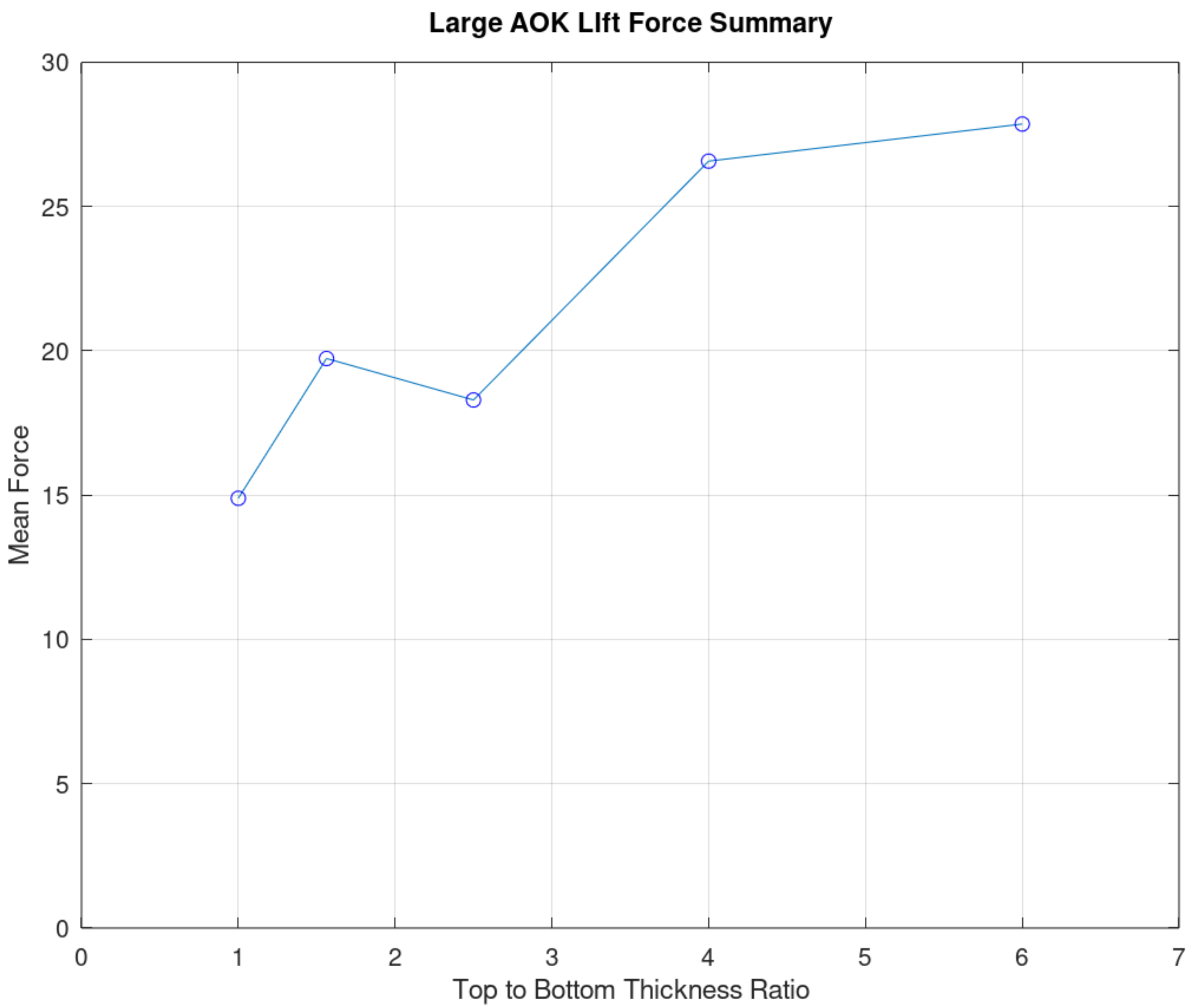

Figure 17: Summary of Large AOK mean lift forces. The connecting lines are only used to facilitate interpretation of the graph, and do not possess any value; only the individual points for each measured airfoil ratio have a true value. The uncertainties for these measured values will be discussed in the Analysis.

	1:1	25:16	5:2	4:1	6:1
Mean Lift Force, g, (+/-)1g	14.893 → 15	19.736 → 20	18.299 → 18	26.575 → 27	27.860 → 28
Standard Deviation, g	1.17	1.88	1.54	1.94	1.66
Signal-to-Noise Ratio	12.78	10.48	11.90	13.70	16.78

Table 3: Mean lift force, standard deviation, and signal-to-noise ratio (SNR) for each airfoil model under the Large AOK.

Data Analysis and Conclusion

Uncertainty

Although the uncertainty for the lift force from the load cell and its calibration is of (+/-) 1g, the real uncertainty is greater than this. This is not because the equipment and measuring tools are faulty, but due to the variation of each run's mean force. After taking more runs (not written in this document), I noticed that the range for the mean force from the graphs above are represented in Figure 18 on the next page.

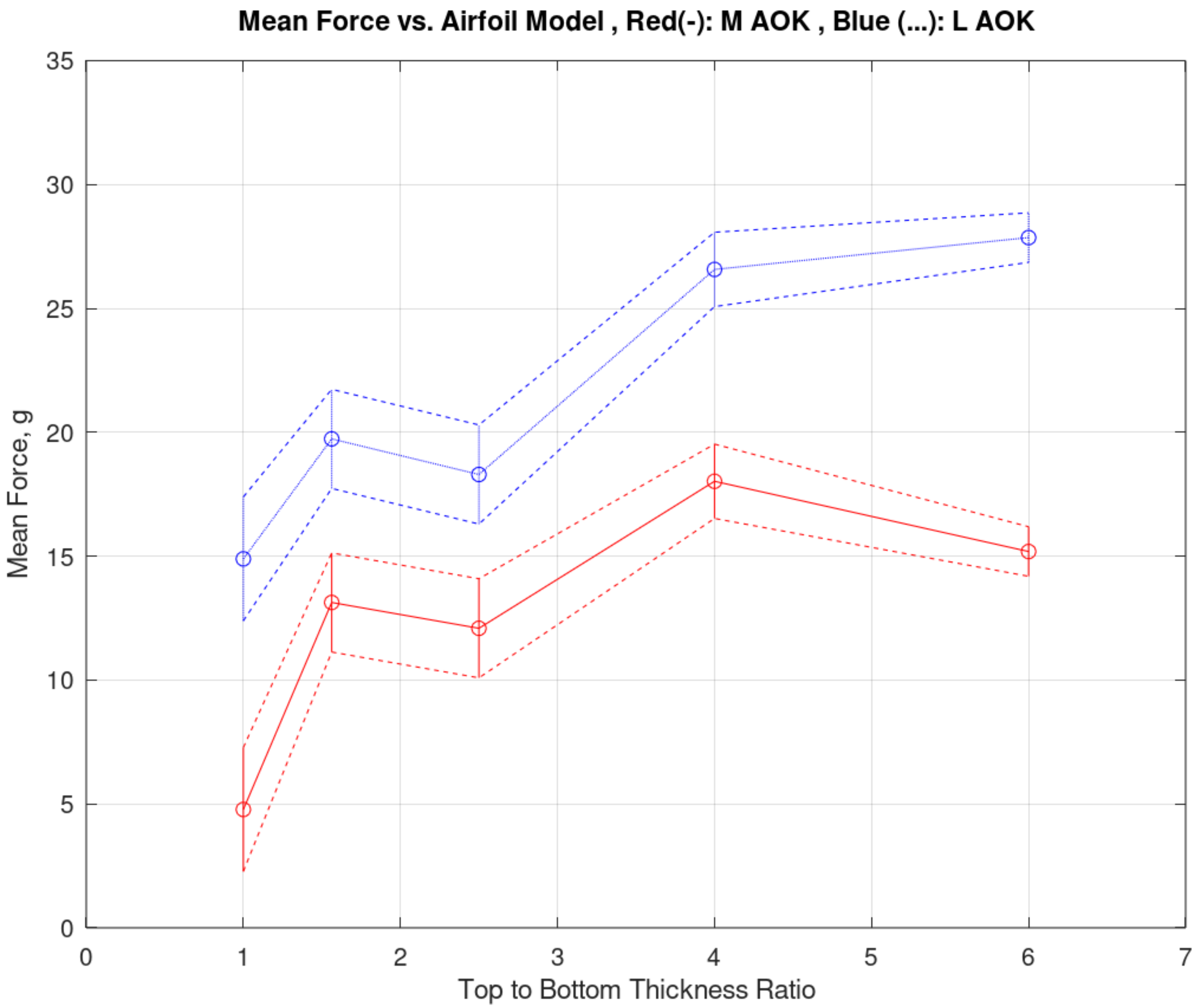

Figure 18: Range for each airfoil model - 1:1 : (+/-) 2.5g , 25:16 and 5:2 : (+/-) 2g , 4:1 : (+/-) 1.5g , 6:1 (+/-)1g

It is important to note that this range is an approximation based on other observations and therefore not simple to quantify. Interestingly, this range in mean values is larger the closer the airfoil's ratio is to one, and smaller as the ratio gets larger.

One reason to this might be that the larger contrast between the pressure on the top and bottom surfaces through a higher ratio provides a smaller gap for variation. Another idea could be that the clamping mechanism and/or shape/disfigurement of the airfoils upon manufacture could affect the mean values as the pressure on each surface is slightly differently.

Summary, Lift Force Pattern, and Sources of Error

The most stable and repeatable airfoils were the 1:1 and 4:1 designs[11] as they maintained the same plotted shape in both the medium and large angles. The 25:16 and 5:2 airfoils have a different pattern than the expected one, that being the 5:2 having a larger lift than the 25:16 model. However, these two are reversed.

This most likely happened because either the 5:2 had systematic error leading to a lower lift force, or the 25:16 had a higher lift force, possibly caused by malfunctions from the cutting process such as uneven surfaces and/or a concave at the tail. Other mechanical errors could also be present.

It is also possible that my prediction was wrong for these 2 airfoils. The issue with this is that when we take the other airfoils into account, the general pattern is for an increase in mean lift force with the ratio. This is especially seen in the large AOK, where the pattern is clearly visible. In the medium AOK set, the 6:1 mean lift is lower than the 4:1. This is very odd, and likely due to random error. In any case, the general pattern, taking into account both datasets and fluctuations in reading, resembles that of a logarithmic function.

[11] Note that for this part of the analysis, I am taking into account the specific points on Figure 18 for each airfoil

Conclusion and Applications

The intent of my research was to find how the lift force of an airfoil varies based on the geometry (i.e., top-to-bottom-thickness ratio) of symmetrical and asymmetrical airfoils. Since the lift force from airfoils parallel to airflow turned out to be negligibly low, I changed the angle of attack, which increases lift force without changing the geometry of the airfoils. To investigate whether the pattern changes with AOK, I used a second angle as well. Although this steers the main purpose of the investigation, I believe it does not harm it. In fact, it gives a more meaningful conclusion, seeing that in a real-life aircraft, lift force is not purely determined by the geometry of the airfoil, but also by how it is used.

The pattern itself resembles a logarithmic function. Although the shape is not perfectly, the general pattern of increasing lift with increased ratio is clearly visible. These findings can be useful in the making of different types of aircraft. For instance, when the main purpose is to carry a large load, an airfoil with a flat bottom is ideal, as this had the greatest contrast between the top and bottom surfaces, producing the most lift out of any ratio. For a supersonic plane, a 1:1 airfoil would be most likely ideal, as it produces no lift when parallel to the wind source, allowing for very high speeds.

Works Cited

Hall, N. (Ed.). (2018, April 5). *Geometry Definitions*. NASA. https://www.grc.nasa.gov/www/k-12/airplane/geom.html.

Benson, T. (Ed.). (2014, June 12). *Wing Geometry Definitions*. NASA. https://wright.nasa.gov/airplane/geom.html.

Designing Smooth Symmetrical Airfoil Wings. Flite Test. (2016, January 29). https://www.flitetest.com/articles/designing-smooth-symmetrical-airfoil-wings.

Wikimedia Foundation. (2020, July 31). *Camber (aerodynamics)*. Wikipedia. https://en.wikipedia.org/wiki/Camber_(aerodynamics).

James. (2017, October 22). *How to Make a Wind Tunnel*. Instructables. https://www.instructables.com/id/How-to-make-a-wind-tunnel/.

Science Buddies. (2020, January 10). *How to Build and Use a Subsonic Wind Tunnel*. Science Buddies. https://www.sciencebuddies.org/science-fair-projects/references/how-to-build-a-wind-tunnel.

HX711 Load Cell Amplifier Interface with Arduino. Circuits4you.com. (2016, November 25). https://circuits4you.com/2016/11/25/hx711-arduino-load-cell/.

Function list. Octave Forge - Function list. https://octave.sourceforge.io/list_functions.php.

Tsokos, K. A. (2014). *Physics for the Ib Diploma*. Cambridge University Press.

Wikimedia Foundation. (2020, September 28). *Analog-to-digital converter*. Wikipedia. https://en.wikipedia.org/wiki/Analog-to-digital_converter.

Wikimedia Foundation. (2020, September 4). *Signal-to-noise ratio*. Wikipedia. https://en.wikipedia.org/wiki/Signal-to-noise_ratio.

Wilson, A. (2016, June 22). *Rigid Foam Insulation and the Environment*. https://www.buildinggreen.com/feature/rigid-foam-insulation-and-environment.

Four Forces of Flight. Science World. https://www.scienceworld.ca/resource/four-forces-flight/